View Article Online / Journal Homepage / Table of Contents for this issue

Reactions of imido complexes of iridium, rhodium and ruthenium

Andreas A. Danopoulos,[a] Geoffrey Wilkinson,*[a] Tracy K. N. Sweet[b] and Michael B. Hursthouse*[b]

[a] *Johnson Matthey Laboratory, Chemistry Department, Imperial College, London SW7 2AY, UK*
[b] *Department of Chemistry, University of Wales Cardiff, PO Box 912, Cardiff CF1 3TB, UK*

Published on 01 January 1996. Downloaded by East Carolina University on 14/09/2015 20:08:20.

Interactions of the known compounds Ir(η-C_5Me_5)(NR) (R = Bu^t **1a** or 2,6-$Pr^i{}_2C_6H_3$ **1b**) with 2,6-xylyl isocyanide [(xyl)NC], mesityl isocyanate and mesityl azide (mesityl = mes = $C_6H_2Me_3$-2,4,6) have been studied. The bridged dimers [Ir(η-C_5Me_5)(μ-NC_5H_9)]$_2$ **2** and [Ir_2(η-C_5Me_5)$_2$(μ-NC_6H_{11})(μ-NHC_6H_{11})]Cl **3** have been synthesized. Reactions of Ru(NR′)($MeC_6H_4Pr^i$-*p*) (R′ = 2,4,6-$Bu^t{}_3C_6H_2$) with (mes)NCO and (mes)N_3 are reported. Attempts to isolate Rh(η-C_5Me_5)(NR) species failed but evidence for Rh(η-C_5Me_5)-[N(2,6-$Pr^i{}_2C_6H_3$)N_3(mes)] was obtained in a trapping reaction in solution using (mes)N_3. The crystal structures of the compounds Ir(η-C_5Me_5)(η^2-Bu^tNCNBu^t)(CNBu^t), [Ir(η-C_5H_5)(μ-NC_5H_9)]$_2$ **2**, **3**, [Ir_2(η-C_5Me_5)(μ-NC_6H_{11})(μ-NHC_6H_{11})]Cl **3**, Ir(η-C_5Me_5)[N(xyl)CHN(2,6-$Pr^i{}_2C_6H_3$)CNC_6H_3(Me)CH_2] **4b**, Ir(η-C_5Me_5)[N(2,6-$Pr^i{}_2C_6H_3$)C(O)N(mes)] **5**, Ir(η-C_5Me_5)[N(2,6-$Pr^i{}_2C_6H_3$)N_3(mes)] **6**, Ru[N(2,4,6-$Bu^t{}_3C_6H_2$)C(O)N(mes)]($MeC_6H_4Pr^i$-*p*) **8** and Ru[N(2,4,6-$Bu^t{}_3C_6H_2$)N_3(mes)]($MeC_6H_4Pr^i$-*p*) **9** have been determined. A reaction mechanism for the formation of **4b** is given.

It was shown[1] that the interaction of the chromium(III) compound Cr(η-C_5Me_5)(=$NC_6H_3Pr^i{}_2$-2,6) generated *in situ*, with an excess of 2,6-xylyl isocyanide in tetrahydrofuran gave the compound shown in diagram **I**. Since the mechanism proposed for the formation involved sequential coupling of three isocyanide molecules it seemed likely that similar insertions into the metal imido bonds could occur with the nucleophilic imido complexes of iridium(III),[2] Ir(η-C_5Me_5)(=NR) (R = Bu^t **1a** or 2,6-$Pr^i{}_2C_6H_3$ **1b**). Reactions of these imido complexes and of the ruthenium(II) complex, Ru(=$NC_6H_2Bu^t{}_3$-2,4,6)(η-$MeC_6H_4Pr^i$-*p*),[3] with 2,6-xylyl isocyanide, (mes)NCO and (mes)N_3 (mes = $C_6H_2Me_3$-2,4,6) are now described. Attempts to obtain rhodium analogues from 'Rh(η-C_5Me_5)(NR)' species made *in situ* were unsuccessful. Physical and analytical data for new compounds are given in Table 1.

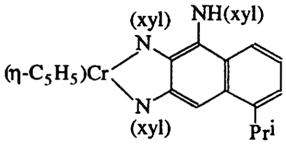

I

Results and Discussion

Iridium complexes

The interaction of compound **1a** with Bu^tNC produces the previously reported carbodiimide compound Ir(η-C_5Me_5)(η^2-Bu^tNCNBu^t)(CNBu^t), whose structural formulation was based on IR and NMR data.[2a] In view of the quite different products obtained when 2,6-xylyl isocyanide is used with either **1a** or **1b** as discussed below, the η^2-carbodiimide structure was confirmed by X-ray diffraction. The structure was solved and successfully refined in the monoclinic space group $P2_1/m$. A diagram of the structure is given in Fig. 1, with selected bond lengths and angles in Table 2. The C_5Me_5 and terminal isocyanide ligands are bisected by the mirror plane, which also contains the metal; it also relates the two Bu^t groups on the carbodiimide. Atom C(20) of this ligand also lies on the mirror plane but the nitrogen N(2) is equally disordered over two sites, thus modelling the asymmetry of the N–C–N grouping arising out of the η^2 C–N bonding. Detailed discussion of the bonding of this ligand is not possible since it was necessary to constrain the positions of the two half-nitrogens to achieve realistic N–C (Bu^t) distances.

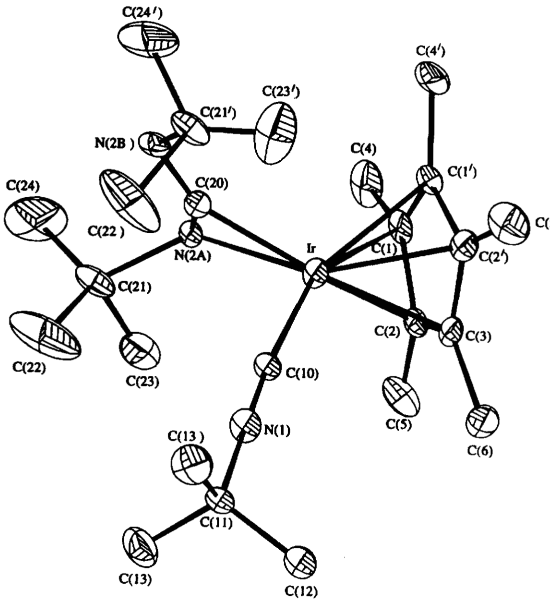

Fig. 1 The structure of Ir(η-C_5Me_5)(η^2-Bu^tNCNBu^t)(CNBu^t). Primed atoms are related to their unprimed equivalents by the crystallographic mirror plane (see text)

In order to find out if carbodiimides were formed in other cases, we first synthesized the cyclopentylimido complex [Ir(η-C_5Me_5)(μ-NC_5H_9)]$_2$ **2** using reaction conditions similar to those described.[2] The structure was confirmed by X-ray diffraction, see Fig. 2 and Table 3. The core geometry is similar to that found for the phenylimido- and 2,6-dimethylphenylimido-bridged dimers described by Dobbs and Bergman[2b] in that the Ir_2N_2 group is folded (dihedral angle between the two IrN_2 planes = 76.14°) and the two nitrogens are not planar [angle sums = 339.8° for N(1) and 351.8° for N(2)]. Possible reasons for these features were discussed previously.[2b] However, the structures show quite significant differences in detail. The Ir • • • Ir distance in **2** is 2.6133(5) Å, some 0.14–0.16 Å shorter than in the aryl derivatives and the

View Article Online

Published on 01 January 1996. Downloaded by East Carolina University on 14/09/2015 20:08:20.

Table 1 Analytical and physical data for new compounds

Compound	M.p./°C	Analysis (%)* C	H	N
2 $[Ir(\eta\text{-}C_5Me_5)(\mu\text{-}NC_5H_9)]_2$	209–211	44.0 (43.9)	6.1 (5.9)	3.2 (3.4)
3 $[Ir_2(\eta\text{-}C_5Me_5)_2(\mu\text{-}NC_6H_{11})(\mu\text{-}NHC_6H_{11})]Cl$	187	43.8 (43.4)	6.0 (6.0)	3.0 (3.2)
4a $Ir(\eta\text{-}C_5Me_5)[N(xyl)CHN(Bu^t)CNC_6H_3(Me)CH_2]$	169–171	58.0 (58.2)	6.2 (6.2)	6.0 (6.4)
4b $Ir(\eta\text{-}C_5Me_5)[N(xyl)CHN(2,6\text{-}Pr^i{}_2C_6H_3)CNC_6H_3(Me)CH_2]$	221–225	61.9 (61.7)	6.4 (6.3)	5.4 (5.3)
5 $Ir(\eta\text{-}C_5Me_5)[N(2,6\text{-}Pr^i{}_2C_6H_3)C(O)N(mes)]$	220	57.9 (57.9)	6.7 (6.9)	4.0 (4.2)
6 $Ir(\eta\text{-}C_5Me_5)[N(2,6\text{-}Pr^i{}_2C_6H_3)N_3(mes)]$	240 (decomp.)	56.2 (56.1)	6.5 (6.5)	8.2 (8.4)
7 $Rh(\eta\text{-}C_5Me_5)[N(2,6\text{-}Pr^i{}_2C_6H_3)N_3(mes)]$	225	64.5 (64.8)	7.5 (7.5)	9.6 (9.8)
8 $Ru[N(2,4,6\text{-}Bu^t{}_3C_6H_2)C(O)N(mes)](MeC_6H_4Pr^i\text{-}p)$	>240	69.5 (69.6)	8.2 (8.2)	4.1 (4.3)
9 $Ru[N(2,4,6\text{-}Bu^t{}_3C_6H_2)N_3(mes)](MeC_6H_4Pr^i\text{-}p)$	98–100	67.7 (67.8)	8.2 (8.2)	8.5 (8.5)

* Calculated values in parentheses. Mass spectral data are given in the Experimental section.

Table 2 Selected bond lengths (Å) and angles (°) for $Ir(\eta\text{-}C_5Me_5)(\eta^2\text{-}Bu^tNCNBu^t)(CNBu^t)$ with estimated standard deviations (e.s.d.s) in parentheses

Ir–Cp(1*)	1.89(2)	N(1)–C(10)	1.137(13)
Ir–C(10)	1.900(10)	N(1)–C(11)	1.430(14)
Ir–C(20)	2.017(9)	C(20)–N(2A)	1.199(13)
Ir–N(2A)	2.206(10)		
Cp(1*)–Ir–C(10)	128.9(7)	C(10)–N(1)–C(11)	178.3(10)
Cp(1*)–Ir–N(2A)	123.3(7)	N(1)–C(10)–Ir	174.6(9)
Cp(1*)–Ir–C(20)	139.4(7)	Ir–N(2A)–C(20)	65.0(7)
C(10)–Ir–N(2A)	99.2(3)	Ir–N(2A)–C(21)	137.4(6)
C(10)–Ir–C(20)	91.8(4)	Ir–C(20)–N(2A)	82.4(7)
N(2A)–Ir–C(20)	32.6(3)	Ir–C(20)–N(2B′)	137.0(6)

Cp(1*) represents the centroid of the C_5Me_5 ring C(1), C(2), C(3), C(1′), C(2′). Primed atoms are related to unprimed ones by the symmetry transformation $x, -y + \frac{1}{2}, z$.

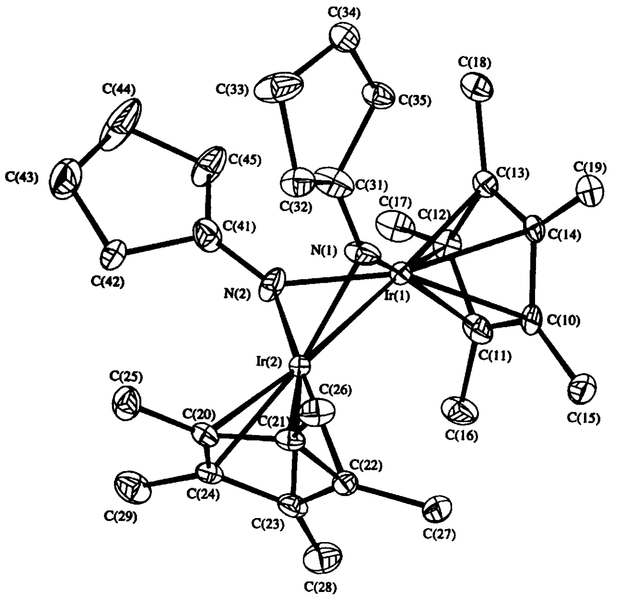

Fig. 2 The structure of $[Ir(\eta\text{-}C_5Me_5)(\mu\text{-}NC_5H_9)]_2$ **2**

Ir–N distances are 2.010–2.046(8) Å, compared with 1.97–1.99(1) Å in the aryls. More importantly, the orientations of the cyclopentyl groups in **2** are both approximately parallel to the Ir ··· Ir vector, whereas in both aryl complexes the rings are perpendicular to this direction. This difference is very significant in that steric interactions between the substituents on the imido functions and the C_5Me_5 groups will be quite different, likely to be much greater in **2**. The resulting steric pressure on the C_5Me_5 groups, which are symmetrically η^5 bound in both complexes, may thus have resulted in the greater folding about the N ··· N vector in **2** leading to a shorter Ir ··· Ir bond.

Table 3 Selected bond lengths (Å) and angles (°) for $[Ir(\eta\text{-}C_5Me_5)(NC_5H_9)]_2$ **2** with e.s.d.s in parentheses

Ir(1) ··· Ir(2)	2.6133(5)	Ir(2)–N(1)	2.049(7)
Ir(1)–N(1)	2.046(8)	Ir(2)–N(2)	2.029(7)
Ir(1)–N(2)	2.010(8)	Ir(2)–Cp(2*)	1.84(2)
Ir(1)–Cp(1*)	1.83(2)		
N(1)–Ir(1)–N(2)	74.4(3)	N(1)–Ir(2)–Cp(2*)	142.9(8)
N(1)–Ir(1)–Cp(1*)	139.9(8)	N(2)–Ir(2)–Cp(2*)	141.8(8)
N(2)–Ir(1)–Cp(1*)	144.2(8)	Ir(1)–N(1)–Ir(2)	79.3(3)
N(1)–Ir(2)–N(2)	74.0(3)	Ir(1)–N(2)–Ir(2)	80.6(3)

Cp(1*) represents the centroid of the C_5Me_5 ring C(10)–C(14), Cp(2*) that of the ring C(20)–C(24).

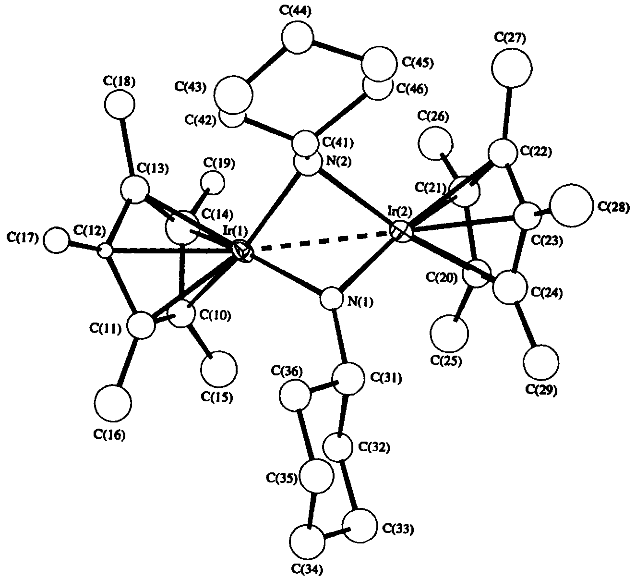

Fig. 3 The structure of the cation $[Ir_2(\eta\text{-}C_5Me_5)_2(\mu\text{-}NC_6H_{11})(\mu\text{-}NHC_6H_{11})]^+$ in **3**

Unfortunately compound **2** was unreactive towards cyclohexyl isocyanide and *tert*-butyl isocyanide even with prolonged refluxing in tetrahydrofuran.

In addition, interaction of $[Ir(\eta\text{-}C_5H_5)Cl_2]_2$ with 3 equivalents of $Li(NHC_6H_{11})$ in thf as above gave low yields of **3**, a dimeric, cationic species with one cyclohexylimido and one cyclohexylamido function. Its identity was established by analytical, spectroscopic (^1H NMR) and crystallographic studies. Although the crystals were of poor quality, the structure determination clearly identifies all main features. A diagram of the cation is shown in Fig. 3, whilst bond lengths and angles are given in Table 4. The dimer cation has the same kind of folded $(C_5Me_5)IrN_2Ir(C_5Me_5)$ feature found for **2**, with differences in detail, as might be expected. The differences in the bridging groups are easily identified, with N(1) the imido

View Article Online

Published on 01 January 1996. Downloaded by East Carolina University on 14/09/2015 20:08:20.

nitrogen giving N–Ir distances of 1.85(3) and 1.92(3) Å, and an angle sum of 356.6°. The amido nitrogen, N(2), gives distances to Ir of 2.02(3) and 2.11(3) Å, and has an angle sum of 319.4°. The cyclohexyl group on the amido is oriented in the 'parallel' mode, whilst that on the imido is roughly in the perpendicular orientation. We presume that the net effect is to reduce steric interactions with the C_5Me_5 groups, since the fold at the N • • • N vector 67.7° is smaller than in **2**, and the Ir • • • Ir bond longer, at 2.724(2) Å.

As noted above compounds **1a** and **1b** show different behaviour when 2,6-xylyl isocyanide is employed. In tetrahydrofuran essentially quantitative (by NMR) yields of the compounds **4a** and **4b** are obtained; both have the structure shown. The structure of **4b** was determined by X-ray diffraction and is shown in Fig. 4; bond lengths and angles are given in Table 5. For the most part the bond lengths and angles in the tridentate ligand are consistent with the formalized structure shown except that the planar amine nitrogen [N(2)] shows some π conjugation with the imine system involving N(3); thus the N(2)–C(101) and C(101)–N(3) distances are both short; N(2)–C(100), however, is similar to a single bond. The presence of the saturated, methylene carbon [C(121)] in the six-membered chelate ring gives this ring some flexibility, so that it is folded at the N(1) • • • C(121) vector and the chelate bite angle is smaller, at 74.8(2)°, than the bite angle [77.1(2)°] in the planar five-membered chelate ring. The Ir–N and Ir–C distances associated with this ligand all indicate normal single bonds. The C_5Me_5 ligand shows slight tilting, with Ir–C distances of 2.186(7)–2.269(6) Å.

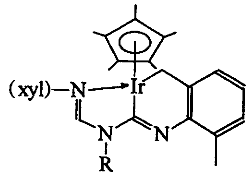

4a R = Bu^t
4b R = 2, 6-Pr$^i{}_2$C$_6$H$_3$

Table 4 Selected bond lengths (Å) and angles (°) for the cation $[Ir_2(\eta\text{-}C_5Me_5)_2(\mu\text{-}NC_6H_{11})(\mu\text{-}NHC_6H_{11})]^+$ in compound **3** with e.s.d.s in parentheses

Ir(1) • • • Ir(2)	2.724(2)	Ir(2)–N(1)	1.85(3)
Ir(1)–N(1)	1.92(3)	Ir(2)–N(2)	2.11(3)
Ir(1)–N(2)	2.02(3)	Ir(2)–Cp(2*)	1.86(10)
Ir(1)–Cp(1*)	1.61(11)		
N(1)–Ir(1)–N(2)	74.0(11)	N(1)–Ir(2)–Cp(2*)	143(3)
N(1)–Ir(1)–Cp(1*)	148(4)	N(2)–Ir(2)–Cp(2*)	144(3)
N(2)–Ir(1)–Cp(1*)	137(4)	Ir(1)–N(1)–Ir(2)	92.6(11)
N(1)–Ir(2)–N(2)	73.2(11)	Ir(1)–N(2)–Ir(2)	82.4(10)

Cp(1*) and Cp(2*) as in Table 3.

Table 5 Selected bond lengths (Å) and angles (°) for $Ir(\eta\text{-}C_5Me_5)[N(xyl)CHN(2,6\text{-}Pr^i{}_2C_6H_3)CNC_6H_3(Me)CH_2]$ **4b** with e.s.d.s in parentheses

Ir–C(121)	2.114(6)	N(2)–C(100)	1.433(7)
Ir–C(100)	2.019(6)	C(100)–N(1)	1.277(7)
Ir–N(3)	2.102(5)	N(1)–C(11)	1.435(7)
Ir–Cp(1*)	1.873(13)	C(11)–C(12)	1.421(8)
N(3)–C(101)	1.303(7)	C(12)–C(121)	1.502(9)
C(101)–N(2)	1.348(8)		
C(121)–Ir–C(100)	74.8(2)	N(3)–C(101)–N(2)	119.4(6)
C(121)–Ir–N(3)	95.0(2)	C(101)–N(2)–C(100)	113.3(5)
C(121)–Ir–Cp(1*)	126.3(6)	N(2)–C(100)–N(1)	113.6(5)
C(100)–Ir–N(3)	77.0(2)	C(100)–N(1)–C(11)	116.4(5)
C(100)–Ir–Cp(1*)	136.0(5)	N(1)–C(11)–C(12)	119.0(5)
N(3)–Ir–Cp(1*)	129.1(5)	C(11)–C(12)–C(121)	119.5(5)
Ir–N(3)–C(101)	112.7(4)	C(12)–C(121)–Ir	109.5(4)

Cp(1*) represents the centroid of the C_5Me_5 ring C(1)–C(5).

The NMR data are consistent with the structure in both cases; assignments of the complicated ^1H spectra were carried out using two-dimensional correlation spectroscopy (COSY). Thus for both compounds **4a** and **4b** the methyl groups on the xylylimino group are diastereotopic giving rise to two separate resonances. The same applies to the methylene protons giving rise to an AB doublet of doublets. In addition, for **4b**, the isopropyl methyls are inequivalent producing four doublets. The resonances of the remaining protons, *e.g.* of the C_5Me_5 groups, methyls on cyclometallated xylyl, aromatics and *tert*-butyl (for **4a**), are in normal positions.

A mechanism for the formation of these compounds is shown in Scheme 1. The first step, a [2 + 2] cycloaddition, is the same as that proposed for the reaction of $Cr(\eta\text{-}C_5Me_5)(=NR)$ with isocyanide[1] and leads to the carbene intermediate **A**. Highly stabilized carbenes of the type shown in diagram **II** are well known in organic chemistry[4a] and as >C:→M donors in

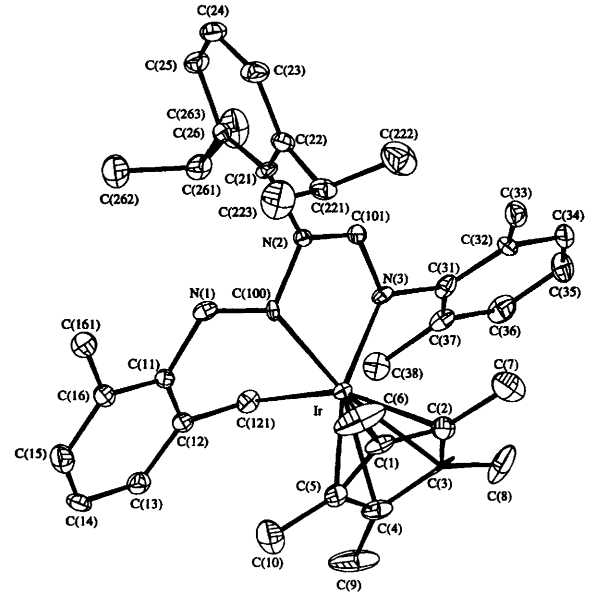

Fig. 4 The structure of $Ir(\eta\text{-}C_5Me_5)[N(xyl)CHN(2,6\text{-}Pr^i{}_2C_6H_3)\text{-}CNC_6H_3(Me)CH_2]$ **4b**

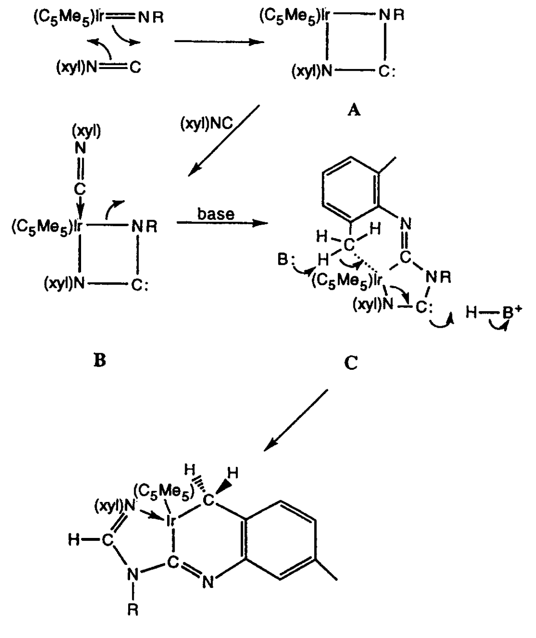

Scheme 1 R = 2,6-Pr$^i{}_2$C$_6$H$_3$

View Article Online

Published on 01 January 1996. Downloaded by East Carolina University on 14/09/2015 20:08:20.

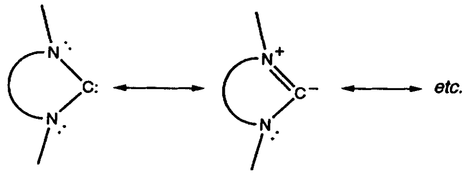

II

Table 6 Selected bond lengths (Å) and angles (°) for Ir(η-C$_5$Me$_5$)[N(2,6-Pr$^i_2$C$_6$H$_3$)C(O)N(mes)] **5** with e.s.d.s in parentheses

Ir–N(1)	1.92(2)	N(1)–C(100)	1.56(2)
Ir–N(2)	2.03(2)	N(2)–C(21)	1.39(2)
Ir–Cp(1*)	1.83(3)	N(2)–C(100)	1.41(3)
N(1)–C(11)	1.27(3)	C(100)–O	1.18(2)
N(1)–Ir–N(2)	68.0(7)	C(21)–N(2)–C(100)	123(2)
N(1)–Ir–Cp(1*)	151.7(1)	Ir–N(2)–C(100)	98.0(13)
N(2)–Ir–Cp(1*)	140.9(11)	Ir–N(2)–C(21)	138.1(14)
C(11)–N(1)–C(100)	116(2)	N(1)–C(100)–N(2)	96(2)
Ir–N(1)–C(100)	97.8(13)	N(1)–C(100)–O	129(2)
Ir–N(1)–C(11)	147(2)	N(2)–C(100)–O	135(2)

Cp(1*) as in Table 5.

complexes of low-valent metals such as Ni^0, Pt^0,[4b] Sm^{II}, Eu^{III}, Yb^{II}[4c] and Pd^{II}.[4d] This step is then followed by isocyanide co-ordination and insertion into the Ir–N$<$ bond to give **B**. Required now is a sequence of transfers as in **C** where a base, presumably the isocyanide, deprotonates the *o*-CH$_3$ group on the xylyl ring leading to formation of the C–CH$_2$–Ir moiety. The hydrogen on B$^+$–H is then transferred to the carbene C atom with concomitant formation of a (xyl)N=C bond and a donor $\ddot{N}$:→Ir bond. There is no change in the oxidation state of iridium in these sequences.

The interaction of the imido compound **1b** with mesityl isocyanate at 110 °C in octane gives moderate yields of the blue, air-stable asymmetric *N*,*N*′-diarylureato[5] complex Ir(η-C$_5$Me$_5$)[N(2,6-Pr$^i_2$C$_6$H$_3$)C(O)N(mes)] **5**. Under similar conditions **1a** with (mes)NCO gives only intractable mixtures; the compound Os^{II}(NBu^t)(MeC$_6$H$_4$Pr^i-*p*) on reaction with Bu^{t}NCO does, however, give a ureato complex.[6]

The structure of compound **5** was determined by X-ray crystallography and is shown in Fig. 5; bond lengths and angles are in Table 6. The crystal quality for this determination was poor, and the resulting accuracy of structural parameters low. Nevertheless the main features are quite clear. The ureate ligand bonds in an almost symmetrical fashion. The Ir–N and Ir–C (C$_5$Me$_5$) distances are very similar to those in the isoelectronic complex Ir(η-C$_5$Me$_5$)[NBu^{t}C(O)O] described by Bergman and co-workers.[2a] The C$_5$Me$_5$ bonding is symmetrical pentahapto in both complexes; in the other ligands the substituents on the N atoms give large Ir–N–C angles ($>$140°) in both cases. However, other parameters indicate that this is a feature of strain (*i.e.* 'bent-bonding overlap') in the Ir–N bonding, arising from the small ligand bite, rather than any steric strain involving the substituent groups and the C$_5$Me$_5$.

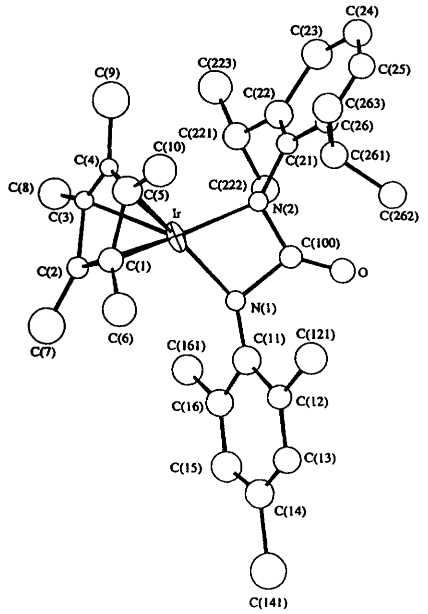

Fig. 5 The structure of Ir(η-C$_5$Me$_5$)[N(2,6-Pr$^i_2$C$_6$H$_3$)C(O)N(mes)] **5**

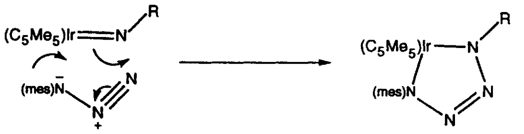

Scheme 2 R = 2,6-Pr$^i_2$C$_6$H$_3$

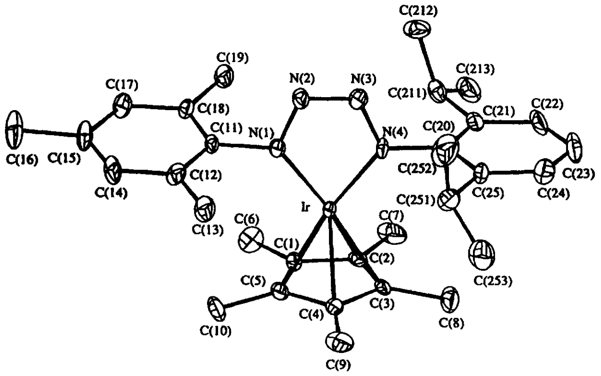

Fig. 6 The structure of Ir(η-C$_5$Me$_5$)[N(2,6-Pr$^i_2$C$_6$H$_3$)N$_3$(mes)] **6**

Table 7 Selected bond lengths (Å) and angles (°) for Ir(η-C$_5$Me$_5$)[N(2,6-Pr$^i_2$C$_6$H$_3$)N$_3$(mes)] **6** with e.s.d.s in parentheses

Ir–N(1)	1.925(5)	N(1)–C(11)	1.451(8)
Ir–N(4)	1.940(5)	N(2)–N(3)	1.277(7)
Ir–Cp(1*)	1.821(14)	N(3)–N(4)	1.367(6)
N(1)–N(2)	1.371(6)	N(4)–C(20)	1.441(8)
N(1)–Ir–N(4)	74.1(2)	N(1)–N(2)–N(3)	112.2(5)
N(1)–Ir–Cp(1*)	143.5(6)	N(2)–N(3)–N(4)	113.0(5)
N(4)–Ir–Cp(1*)	142.5(6)	N(3)–N(4)–C(20)	113.0(5)
N(2)–N(1)–C(11)	111.2(5)	N(3)–N(4)–Ir	119.9(4)
Ir–N(1)–C(11)	127.9(4)	C(20)–N(4)–Ir	127.0(4)
Ir–N(1)–N(2)	120.8(4)		

Cp(1*) as in Table 5.

The interaction of compound **1b** with mesityl azide in tetrahydrofuran (thf) at room temperature produces the *N*,*N*′-diaryltetrazene[7] complex **6** by the usual 1,3-dipolar cycloaddition in Scheme 2. The structure determined by X-ray diffraction is shown in Fig. 6; bond lengths and angles are in Table 7. The five-membered IrN$_4$ ring has almost equal Ir–N bond lengths and although the double bond seems to be localized at N(2)–N(3) [1.277(7) Å], N(1) and N(4) are planar while the N(1)–N(2) and N(3)–N(4) distances are slightly shorter than expected for normal single bonds; this indicates some electron delocalization over the four N atoms. The C$_5$Me$_5$ ligand bonds symmetrically, with Ir–C distances differing only by 0.02 Å. The ^{1}H NMR spectrum has bands for mesityl and 2,6-disopropylphenyl groups in a 1 : 1 ratio and the isopropyl methyl groups are diastereotopic, as found for **5**. The electron impact (EI) mass spectrum shows the molecular ion. There is no sign of cleavage of the tetrazene moiety thermally or on photolysis even in the presence of donors such as PMe$_3$. Tetrazene osmium complexes

View Article Online

Published on 01 January 1996. Downloaded by East Carolina University on 14/09/2015 20:08:20.

have been obtained by reaction of Os(NBu^t)(MeC$_6$H$_4$Pr^i-*p*) with azides.[6]

Rhodium complexes

Attempts to isolate rhodium analogues of **1a** and **1b** have failed. At temperatures above *ca.* 5 °C the red-brown solutions from the reactions of [Rh(η-C$_5$Me$_5$)Cl$_2$]$_2$[8] and various lithium amido compounds, Li(NHR) (R = alkyl and aryl), that may possibly contain Rh(η-C$_5$Me$_5$)(NR) species, decomposed to give purple solutions which on evaporation leave solids giving purple solutions in hexane. Crystals could not be obtained from a range of solvents. The NMR spectra were uninterpretable and addition of compounds such as tertiary phosphines, pyridine, *etc.*, gave no identifiable adducts. Attempts to isolate Rh(η-C$_5$Me$_5$)(NR) species at low temperatures in polar or non-polar solvents also failed.

The only indication that Rh(η-C$_5$Me$_5$)(C$_6$H$_3$Pr$^i{}_2$-2,6) could exist, for a short time at any rate at 0 °C, was the interaction with (mes)N$_3$ immediately after generation which produced the rhodium tetrazene complex **7**, which is analogous to that of iridium and has similar spectroscopic properties. The yellow-brown crystalline product was air-stable; the mass spectrum showed the molecular ion. The cobalt analogue Co(η-C$_5$Me$_5$)[(mes)N$_4$(2,6-Pr$^i{}_2$C$_6$H$_3$)] has been made similarly by H. Petersen in these laboratories.

We have also tried to obtain imido species starting with other materials: [Rh(η-C$_5$H$_5$)Cl$_2$]$_n$,[9a] {Rh[HB(dmpz)$_3$]Cl$_2$}$_2$[9b] (dmpz = 3,5-dimethylpyrazolyl), Rh(η-C$_5$Me$_5$)(Me)Br(PMe)$_3$[9c] and Rh(η-C$_5$Me$_5$)(PMe$_3$)(O$_3$SCF$_3$)$_2$[9d] under a variety of conditions with the lithium salts from NH$_2$Bu^t and several aromatic amines, but in all cases intractable materials were obtained.

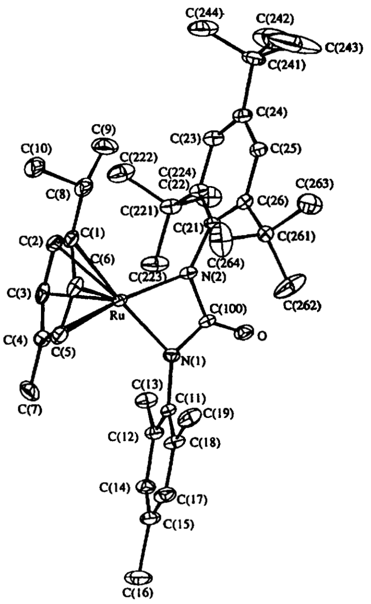

Fig. 7 The structure of Ru[N(2,4,6-Bu$^t{}_3$C$_6$H$_2$)C(O)N(mes)](MeC$_6$H$_4$Pr^i-*p*) **8**

The reason for the difference in stability or reactivity of the rhodium and iridium compounds is not clear; possibly reduction to unstable or polymeric species is occurring with the rhodium compounds.

Ruthenium complexes

The interaction of Ru(NR)(MeC$_6$H$_4$Pr^i-*p*), R = 2,4,6-Bu$^t{}_3$C$_6$H$_2$,[3] with (mes)NCO at room temperature shows that this complex is more reactive than the iridium(III) species. The asymmetric ureato complex **8** is obtained as thermally and air-stable blue crystals. The crystal structure is shown in Fig. 7; bond lengths and angles are in Table 8. The structure is as expected, but with small deviations from idealized geometry arising out of some degree of steric strain involving the Pr^i group on the cymene and Bu^t groups on the ureate ligand. Thus the cymene ring is tilted slightly, with Ru–C distances varying from 2.139(5) [C(3)] to 2.265(5) Å [C(1)], and Ru–N(2) is some 0.035 Å longer than the Ru–N(1) bond length. The Ru–N(2)–C(21) angle to the R substituent is also *ca.* 5° greater than the equivalent angle Ru–N(1)–C(11), but both are some 10–15° smaller than in the iridium complex **5**. The N–C distances in the ureate ligand are equal.

The interaction of Ru(NR)(MeC$_6$H$_4$Pr^i-*p*), R = 2,4,6-Bu$^t{}_3$C$_6$H$_2$, with (mes)N$_3$ gave a yellow-brown tetrazene complex **9**, characterized by analytical and ^{1}H NMR data. The latter show distinct resonances for mesityl and R groups while the aromatic protons of the η^6-arene ring appear as a doublet of doublets (AB) indicating that the asymmetric structure is not present in solution, probably because of η^6-arene ring rotations. The solid-state structure is shown in Fig. 8 and bond lengths and angles are given in Table 9.

The structure and geometry are as expected, in view of the

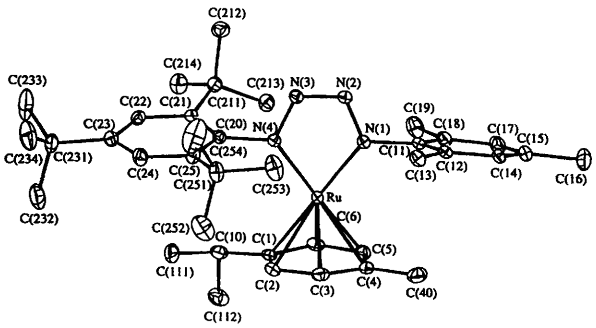

Fig. 8 The structure of Ru[N(2,4,6-Bu$^t{}_3$C$_6$H$_2$)N$_3$(mes)](MeC$_6$H$_4$Pr^i-*p*) **9**

Table 8 Selected bond lengths (Å) and angles (°) for Ru[N(2,4,6-Bu$^t{}_3$C$_6$H$_2$)C(O)N(mes)](MeC$_6$H$_4$Pr^i-*p*) **8** with e.s.d.s in parentheses

Ru–N(1)	1.988(4)	N(1)–C(100)	1.408(6)
Ru–N(2)	2.023(4)	N(2)–C(21)	1.434(6)
Ru–Cym(1*)	1.681(10)	N(2)–C(100)	1.390(6)
N(1)–C(11)	1.411(6)	C(100)–O	1.218(5)
N(1)–Ru–N(2)	66.1(2)	C(21)–N(2)–C(100)	127.5(4)
N(1)–Ru–Cym(1*)	143.8(4)	Ru–N(2)–C(100)	94.2(3)
N(2)–Ru–Cym(1*)	149.8(4)	Ru–N(2)–C(21)	138.0(3)
C(11)–N(1)–C(100)	128.1(4)	N(1)–C(100)–N(2)	102.8(4)
Ru–N(1)–C(100)	95.2(3)	N(1)–C(100)–O	127.3(4)
Ru–N(1)–C(11)	133.5(3)	N(2)–C(100)–O	129.8(4)

Cym(1*) represents the centroid of the cymene ring C(1)–C(6).

Table 9 Selected bond lengths (Å) and angles (°) for Ru[N(2,4,6-Bu$^t{}_3$C$_6$H$_2$)N$_3$(mes)](MeC$_6$H$_4$Pr^i-*p*) **9** with e.s.d.s in parentheses

Ru–N(1)	1.946(3)	N(1)–C(11)	1.439(4)
Ru–N(4)	1.967(3)	N(2)–N(3)	1.288(4)
Ru–Cym(1*)	1.709(8)	N(3)–N(4)	1.358(3)
N(1)–N(2)	1.365(4)	N(4)–C(20)	1.444(4)
N(1)–Ru–N(4)	74.08(11)	N(1)–N(2)–N(3)	112.6(2)
N(1)–Ru–Cym(1*)	140.5(3)	N(2)–N(3)–N(4)	113.7(2)
N(4)–Ru–Cym(1*)	145.4(3)	N(3)–N(4)–C(20)	111.4(2)
N(2)–N(1)–C(11)	112.3(2)	N(3)–N(4)–Ru	119.2(2)
Ru–N(1)–C(11)	127.0(2)	C(20)–N(4)–Ru	129.3(2)
Ru–N(1)–N(2)	120.4(2)		

Cym(1*) as in Table 8.

Published on 01 January 1996. Downloaded by East Carolina University on 14/09/2015 20:08:20.

earlier work on complexes **6** and **7**. The cymene ring is again slightly tilted, with Ru–C distances ranging from 2.170(4) to 2.270(3) Å, the longest to C(1), which is also bound to a Pr^i substituent. It is interesting that the orientation of the cymene ring, which appears to be fluxional in solution, places the Pr^i group on the same side as the bulky R substituent, as in complex **6**. The structure of the ruthenium–tetrazene ring is analogous to that found in **6**, with the double bond localized at N(2)–N(3).

The interaction of $Ru(NR)(MeC_6H_4Pr^i$-*p*) with isocyanides is very fast even in non-polar solvents like light petroleum and at low temperatures (−78 °C) as judged by changes in the solution from green to brown. Since crystalline products could not be obtained, the reaction with Bu^tNC in [$^2H_8$]toluene was followed by ^1H NMR spectra. Initially a species is formed instantaneously at −60 °C that has one Bu^tNC per ruthenium. Shifts are observed for protons assignable to Bu^t, arylimido and η^6-arene groups. This species begins to disappear at 0 °C being replaced by that of the final product (or products). The presence of more than one Bu^tNC resonance precludes any reliable conclusions on the nature of the product(s) and no crystals could be isolated.

Experimental

Analyses were by the Imperial College microanalytical laboratory. All operations were carried out under purified Ar or N_2, under vacuum or in a Vacuum Atmospheres glove-box. General techniques have been described.[10]

The NMR data were obtained on a JEOL EX-270 or a Bruker Avance DRX 300 spectrometer operating at 270 and 300 MHz (^1H) respectively and referenced to the residual ^1H impurity in the solvent (δ 7.15, C_6D_6; 7.26, $CDCl_3$). Mass spectra were recorded using VG-7070E (EI) and V. G. Autospec spectrometers. Commercial chemicals were from Aldrich and Fluka. The light petroleum used had b.p. 40–60 °C.

Mesityl isocyanate[11] and mesityl azide[12] were made as referenced.

Bis[(μ-cyclopentylmido)(η-pentamethylcyclopentadienyl)-iridium(III)] 2

To a solution of $[Ir(\eta\text{-}C_5Me_5)Cl_2]_2$ in thf (0.3 g, 0.37 mmol in 30 cm^3) at −78 °C was added a solution of $Li(NHC_5H_9)$ (0.14 g, 1.5 mmol) in thf (*ca.* 10 cm^3). The reaction suspension was allowed to warm to room temperature and stirred for 2 h giving an orange solution. Evaporation of volatiles under reduced pressure, extraction of the residue in hot light petroleum (3 × 30 cm^3), filtration and concentration of extracts and cooling (−20 °C) gave orange prisms. Yield: 0.1 g, *ca.* 35%. NMR (C_6D_6): ^1H, δ 2.1 (s, 30 H, C_5Me_5), 1.2, 1.5, 1.8 and 2.5 (groups of broad multiplets, 18 H, C_5H_9N).

μ-(Cyclohexylamido)-μ-(cyclohexylimido)-bis(η-pentamethyl-cyclopentadienyl)diiridium(III) chloride 3

To a solution of $[Ir(\eta\text{-}C_5Me_5)Cl_2]_2$ (0.3 g, 0.37 mmol) in thf (*ca.* 30 cm^3) at −78 °C was added a solution of $Li(NHC_6H_{11})$ (0.12 g, 1.1 mmol) in thf (*ca.* 10 cm^3). The suspension was allowed to warm to room temperature and stirred for 1 h giving a yellow-orange solution. Evaporation of volatiles under reduced pressure, extraction of the residue in hot light petroleum (3 × 30 cm^3), filtration, concentration of extracts and cooling (−20 °C) gave orange crystals. Yield: 0.08 g, 25%. NMR (C_6D_6): ^1H, δ 10.6 [s br, 1 H, N*H*(C_6H_{11})], 2.0 (s, 30 H, C_5Me_5) and 1.8–1.2 (m, 22 H, C_6H_{11}).

Interaction of $Ir(\eta\text{-}C_5Me_5)(NBu^t)$ with 2,6-xylyl isocyanide to give compound 4a

To a solution of $Ir(\eta\text{-}C_5Me_5)(NBu^t)$ (0.25 g, 0.63 mmol) in thf (20 cm^3) was added a solution of xylyl isocyanide (0.25 g, 1.9 mmol) in thf (15 cm^3). The yellow-orange reaction mixture was refluxed for 2 h and the volatiles removed under reduced pressure. The yellow-orange residue was recrystallized from hot light petroleum. Yield: 0.3 g, 72%. Mass spectrum (EI): *m/z* 660 (M^+ + 1) and 604 (M^+ + 1 − isobutylene). NMR (C_6D_6): ^1H, δ 7.5–7.0 (m, 6 H, aromatic), 3.0 and 2.5 (d, 2 H, $IrCH_2C_6H_3Me$), 2.75, 2.51 and 2.1 (s, 3 H each, xylyl methyl), 1.47 (s, 9 H, $NCMe_3$) and 1.33 (s, 15 H, C_5Me_5).

Interaction of $Ir(\eta\text{-}C_5Me_5)(NC_6H_3Pr^i_2\text{-}2,6)$ with 2,6-xylyl isocyanide to give compound 4b

Compound **4b** was prepared as for **4a** from $Ir(\eta\text{-}C_5Me_5)(NC_6H_3Pr^i_2\text{-}2,6)$ (0.3 g, 0.6 mmol) and 2,6-xylyl isocyanide (0.24 g, 1.8 mmol). After evaporating the thf solution the yellow residue was recrystallized from diethyl ether. Yield: 0.37 g, 80%. Mass spectrum (EI): *m/z* 765 (M^+ + 1) and 635 [M^+ + 1 − $C_6H_3(Me)CH_2$]. NMR (C_6D_6): ^1H, δ 7.6–6.90 (m, 9 H, aromatic), 3.60 and 3.10 (spt, 1 H each, Me_2CH), 3.40 and 2.55 (doublet of doublets, 2 H, $IrCH_2C_6H_3Me$), 2.45, 2.40 and 2.0 (s, 3 H each, xylyl methyl), 1.65, 1.40, 1.15 and 1.00 (d, 3 H each, Me_2CH) and 1.38 (s, 15 H, C_5Me_5).

[*N*-(2,6-Diisopropylphenyl)-*N*′-(2,4,6-trimethylphenyl)-ureato](η-pentamethylcyclopentadienyl)iridium(III) 5

A solution of compound **1b** (0.25 g, 0.5 mmol) and (mes)NCO 0.1 g, (*ca.* 0.6 mmol) in octane was heated at 110 °C for 48 h. After removal of octane under reduced pressure the blue residue was recrystallized from light petroleum to yield 0.21 g (*ca.* 65%) of green-blue **5**. NMR (C_6D_6): ^1H, δ 7.3 (m, 3 H, aromatic), 6.9 (s, 2 H, aromatic), 3.8 (spt, 2 H, C*H*Me_2), 2.6 (s, 6 H, *o*-Me), 2.3 (s, 3 H, *p*-Me), 1.45 (doublet of doublets, 12 H, CHMe_2) and 1.05 (s, 15 H, C_5Me_5). IR (Nujol): 1650 cm^{-1} [ν(C=O)].

[1-(2,6-Diisopropylphenyl)-4-(2,4,6-trimethylphenyl)-tetrazene-1,4-diyl](η-pentamethylcyclopentadienyl)iridium(III) 6

To a solution of compound **1b** (0.25 g, 0.5 mmol) in thf (20 cm^3) was added *via* cannula a thf solution of $(mes)N_3$ (0.1 g, 0.6 mmol in 5 cm^3). The yellow reaction solution was stirred at room temperature for 12 h. Removal of volatiles under reduced pressure and crystallization of the residue from light petroleum gave yellow needles. Yield: 0.28 g, 85%. Mass spectrum (EI): *m/z* 636 (M^+ − 28) and 622 (M^+ − 42). NMR (C_6D_6): ^1H, δ 7.3 (m, 3 H, aromatic), 6.9 (s, 2 H, aromatic), 3.3 (spt, 2 H, C*H*Me_2), 2.4 (s, 3 H, *p*-Me), 2.2 (s, 6 H, *o*-Me), 1.4 (doublet of doublets, 12 H, CHMe_2) and 1.30 (s, 15 H, C_5Me_5).

[1-(2,6-Diisopropylphenyl)-4-(2,4,6-trimethylphenyl)tetrazene-1,4-diyl](η-pentamethylcyclopentadienyl)rhodium(III) 7

To a mixture of $[Rh(\eta\text{-}C_5Me_5)Cl_2]_2$ in thf (0.25 g, 0.4 mmol in 30 cm^3) at −78 °C was added a solution of $Li[NH(C_6H_3Pr^i_2\text{-}2,6)]$ (0.3 g, 1.62 mmol) in thf (10 cm^3). The suspension was allowed to warm to 0 °C when all solids dissolved. Stirring at this temperature was continued for *ca.* 0.5 h and the red-brown reaction mixture was cooled again to −78 °C and a solution of $(mes)N_3$ (0.07 g) in thf (5 cm^3) was added dropwise *via* cannula. After completion of the addition the reaction mixture was allowed to warm and stirred at room temperature for 0.5 h. Removal of volatiles under reduced pressure, followed by extraction of volatiles with light petroleum (3 × 30 cm^3), filtration, concentration to *ca.* 25 cm^3 and cooling gave yellow-brown crystals. Yield: 0.1 g, 45%. Mass spectrum (EI): *m/z* 574 (M^+) and 546 (M^+ − N_2). NMR (C_6D_6): ^1H, δ 7.4 (m, 3 H, aromatic), 6.9 (s, 2 H, aromatic), 3.2 (spt, 2 H, C*H*Me_2), 2.4 (s, 3 H, *p*-Me), 2.2 (s, 6 H, *o*-Me), 1.4 (doublet of doublets, 12 H, CHMe_2) and 1.30 (s, 15 H, C_5Me_5).

Published on 01 January 1996. Downloaded by East Carolina University on 14/09/2015 20:08:20.

Table 10 Crystal data and structure refinement details for the carbodiimide and compounds **2**, **3**, **4b**, **5**, **6**, **8** and **9**

		2	**3**	**4b**	**5**	**6**	**8**	**9**
Formula	$C_{24}H_{42}IrN_3$	$C_{30}H_{48}Ir_2N_2$	$C_{32}H_{53}ClIr_2N_2$	$C_{40}H_{50}IrN_3$	$C_{32}H_{43}IrN_2O$	$C_{31}H_{43}IrN_4$	$C_{38}H_{54}N_2ORu\cdot 0.5C_5H_{12}$	$C_{37}H_{54}N_4Ru\cdot 0.5C_5H_{12}$
M_r	564.84	821.10	885.61	765.03	663.90	663.89	691.98	691.98
Crystal system	Monoclinic	Orthorhombic	Monoclinic	Monoclinic	Triclinic	Trigonal	Monoclinic	Monoclinic
Space group	$P2_1/m$	$Pbca$	$P2_1/n$	$P2_1/n$	$P\bar{1}$	$R\bar{3}$	$P2_1/c$	$P2_1/c$
a/Å	9.708(1)	21.836(1)	12.036(6)	9.811(6)	8.58(1)	42.90(2)	9.487(6)	9.203(5)
b/Å	15.001(2)	17.266(4)	21.539(10)	17.068(8)	11.22(3)	42.90(2)	14.579(9)	14.373(8)
c/Å	9.965(1)	15.480(3)	12.388(1)	21.174(10)	15.91(3)	8.400(1)	28.283(6)	28.699(7)
α/°					83.51(6)			
β/°	118.67(1)		93.70(3)	94.99(8)	87.89(7)		95.11(3)	94.85(6)
γ/°					79.4(2)	120		
U/Å^3	1273(2)	5836(2)	3205(2)	3532(3)	1496(5)	13 388(9)	3896(4)	3783(3)
Z	2	8	4	4	2	18	4	4
D_c/Mg m^{-3}	1.473	1.869	1.835	1.439	1.474	1.482	1.180	1.215
F(000)	568	3168	1720	1552	668	6012	1476	1476
Crystal colour	Beige	Pale orange	Orange	Yellow	Turquoise	Yellow	Turquoise	Orange
Crystal size/mm	0.24 × 0.09 × 0.05	0.48 × 0.24 × 0.09	0.15 × 0.12 × 0.06	0.12 × 0.12 × 0.09	0.12 × 0.09 × 0.02	0.48 × 0.05 × 0.03	0.36 × 0.30 × 0.18	0.42 × 0.39 × 0.18
μ(Mo-Kα)/mm^{-1}	5.075	8.815	8.114	3.680	4.334	4.357	0.402	0.445
Reflections collected	5329	16 082	9459	12 543	5920	16 563	14 434	11 565
Independent reflections (R_{int})	1993, 0.0852	4474, 0.0896	4580, 0.1851	5301, 0.0563	4029, 0.1311	4605, 0.0606	5566, 0.0832	5439, 0.0685
Maximum, minimum correction factors	1.289, 0.840	1.881, 0.756	1.241, 0.715	1.042, 0.870	1.359, 0.769	1.139, 0.876	1.151, 0.735	1.117, 0.841
Data, restraints, parameters	1991, 0, 156	4471, 0, 317	4577, 0, 174	5298, 0, 453	4025, 0, 162	4602, 0, 365	5562, 0, 437	5433, 0, 431
Goodness of fit, F^2	0.985	1.051	0.994	0.732	0.700	0.815	0.986	1.026
Observed data [$I > 2\sigma(I)$]	1597	3764	2483	3502	1500	3322	4111	4894
$R1$, $wR2$ [$I > 2\sigma(I)$]	0.0440, 0.0979	0.0471, 0.1064	0.1162, 0.2590	0.0312, 0.0559	0.0762, 0.1519	0.0311, 0.0600	0.0541, 0.1290	0.0495, 0.1231
(all data)	0.0550, 0.1025	0.0549, 0.1114	0.1827, 0.2899	0.0613, 0.0613	0.1612, 0.1930	0.0552, 0.0648	0.0743, 0.1377	0.0544, 0.1284
Largest difference peak and hole/e Å^{-3}	1.717, −1.118	7.436, −2.015	8.687, −3.509	1.868, −0.607	1.784, −1.352	3.797, −0.612	1.349, −0.543	2.150, −0.549

$S = [\Sigma w(F_o^2 - F_c^2)^2/(n - p)]^{\frac{1}{2}}$, $R1 = \Sigma[(F_o - F_c)]/\Sigma F_o$, $wR2 = [\Sigma w(F_o^2 - F_c^2)^2/\Sigma w(F_o^2)^2]^{\frac{1}{2}}$, $w = 1/[\sigma^2(F_o^2) + (xP)^2 + gP]$ and $P = [\max(F_o^2) + 2(F_c^2)]/3$, where n = number of reflections and p = total number of parameters, x = 0.0524, 0.0615, 0.1220, 0, 0.0188, 0.0058, 0.0670 and 0.1018 for the carbodiimide and compounds **2**, **3**, **4b**, **5**, **6**, **8** and **9** respectively and g = 0 in each case.

View Article Online

Published on 01 January 1996. Downloaded by East Carolina University on 14/09/2015 20:08:20.

η^6-(*p*-Cymene)[*N*-(2,4,6-tri-*tert*-butylphenyl)-*N'*-(2,4,6-trimethylphenyl)ureato]ruthenium(II) 8

To a solution of (*p*-cymene)(2,4,6-tributylphenylimido)ruthenium[3] in thf (0.3 g, 0.61 mmol in 20 cm^3) at room temperature was added a solution of (mes)NCO (0.1 g, 0.65 mmol) in thf (10 cm^3). The green solution became green-brown and after stirring at room temperature for *ca.* 2 h, evaporation of volatiles under reduced pressure, extraction of the residue with light petroleum (2 × 20 cm^3), filtration, concentration of filtrates (to *ca.* 5 cm^3) and cooling (−20 °C) gave blue crystals. Yield: 0.14 g, 40%. Mass spectrum (FAB): *m*/*z* 665 (M^+) and 503 [M^+ − (mes)NHCO]. NMR (C_6D_6): ^{1}H, δ 7.6 (s, 2 H, aromatic), 6.9 (s, 2 H, aromatic), 4.6–4.4 (doublet of doublets, 4 H, η^6-$Pr^iC_6\mathit{H}_4Me$), 2.6 (s, 6 H, *o*-$\mathit{Me}_2C_6H_2Me$), 2.3 (s, 3 H, *p*-$\mathit{Me}C_6H_2Me_2$), 1.8 (s, 18 H, *o*-$\mathit{Bu}^t{}_2C_6H_2Bu^t$), 1.4 (s, 9 H, *p*-$Bu^tC_6H_2\mathit{Bu}^t{}_2$) and 0.7 (d, 6 H, η^6-$\mathit{Pr}^iC_6H_4Me$). IR (Nujol): 1655 cm^{-1} [ν(C=O)].

η^6-(*p*-Cymene)[1-(2,4,6-tri-*tert*-butylphenyl)-4-(2,4,6-trimethylphenyl)tetrazene-1,4-diyl]ruthenium(II) 9

To a solution of (*p*-cymene)(2,4,6-tri-*tert*-butylphenylimido)ruthenium in light petroleum (0.3 g, 0.61 mmol in 40 cm^3) at −78 °C was added a solution of (mes)N_3 in the same solvent (0.1 g, 0.65 mmol in 20 cm^3). The green solution, which became brown between −78 and 0 °C, was stirred at room temperature for *ca.* 2 h. Evaporation of volatiles under reduced pressure, extraction of the residue with light petroleum (2 × 20 cm^3), filtration, concentration of filtrates (to *ca.* 10 cm^3) and cooling (−20 °C) gave yellow-brown crystals. Yield: 0.22 g, 55%. Mass spectrum (EI): *m*/*z*, 495 [M^+ − (mes)N_3]. NMR (C_6D_6): ^{1}H, δ 7.5 and 6.8 (s, 2 H each, aromatic), 4.8–4.5 [doublet of doublets, 4 H, η^6-$C_6\mathit{H}_4(Me)Pr^i$], 2.3 (s, 3 H, *p*-$\mathit{Me}C_6H_2Me_2$), 2.1 (s, 6 H, *o*-$\mathit{Me}_2C_6H_2Me$), 2.0 [spt, 1 H, η^6-$C_6H_4(Me)C\mathit{H}Me_2$], 1.5 (s, 9 H, *p*-$\mathit{Bu}^tC_6H_2Bu^t{}_2$), 1.4 (s, 3 H, η^6-$\mathit{Me}C_6H_4Pr^i$), 1.3 (s, 18 H, *o*-$\mathit{Bu}^t{}_2C_6H_2Bu^t$) and 0.7 [d, 6 H, η^6-$C_6H_4Me(CH\mathit{Me}_2)$].

X-Ray crystallography

X-Ray data for all of the compounds were collected at 150 K. A FAST TV area detector diffractometer with Mo-Kα radiation (λ = 0.710 69 Å) was employed, as previously described.[13] The structures of compounds **2**, **6** and **8** were solved using the PATT instruction of SHELXS 86,[14] whilst those of the carbodiimide and **3**, **4b**, **5** and **9** were solved *via* direct methods procedures of the same program. They were refined by full-matrix least squares on $F_o{}^2$, using the program SHELXL 93.[15] All data used were corrected for Lorentz-polarization factors, and subsequently for absorption using the program DIFABS[16] with maximum and minimum correction factors listed in Table 10. The non-hydrogen atoms of the carbodiimide and compounds **2**, **4b** and **6** were refined with anisotropic thermal parameters. Compounds **3** and **5** exhibited fragile crystals of platy morphology which gave rise to poor-quality data, therefore only the heavy atoms of these structures were anisotropically refined. The non-hydrogen atoms of **8** and **9** were refined with anisotropic thermal parameters, except for the carbon atoms of the highly disordered solvate molecules, originating from light petroleum, and identified as pentane in both compounds. The hydrogen atoms of the solvate molecules in **8** and **9** were ignored. The phenyl hydrogen atoms of **8** and **9** were experimentally located whilst the remainder were placed in idealized positions. The phenyl and isopropyl hydrogen atoms of **4b** and **6** were experimentally located, whilst the remaining hydrogen atom positions were again calculated. All of the hydrogen atoms in the carbodiimide and compounds **2**, **3** and **5** were included in idealized positions. Compounds **2** and **3** exhibit large residual peaks in the difference map which lie in the vicinity of the metal atoms. This arises from poor-quality data in the latter case, and due to a slight twinned component in crystals of the former. The equations used in the refinement, the weighting scheme and parameters employed for each compound are included as a footnote to Table 10.

Atomic coordinates, thermal parameters and bond lengths and angles have been deposited at the Cambridge Crystallographic Data Centre (CCDC). See Instructions for Authors, *J. Chem. Soc., Dalton Trans.*, 1996, Issue 1. Any request to the CCDC for this material should quote the full literature citation and the reference number 186/186.

Acknowledgements

We thank the EPSRC for support (to A. A. D.) and provision of X-ray facilities. We are indebted to Johnson Matthey plc for loan of platinum group metals and to Professor W. B. Motherwell for discussions.

References

1 A. A. Danopoulos, G. Wilkinson, T. K. N. Sweet and M. B. Hursthouse, *J. Chem. Soc., Dalton Trans.*, 1996, 271.

2 (*a*) D. S. Glueck, J. Wu, F. J. Hollander and R. G. Bergman, *J. Am. Chem. Soc.*, 1991, **113**, 2041; (*b*) D. A. Dobbs and R. G. Bergman, *Organometallics*, 1994, **13**, 4594.

3 A. K. Burrell and A. J. Steedman, *J. Chem. Soc., Chem. Commun.*, 1995, 2109.

4 (*a*) R. R. Savers, *Tetrahedron Lett.*, 1996, **37**, 149; A. J. Arduengo, III, J. R. Goerlich and W. J. Marshall, *J. Am. Chem. Soc.*, 1995, **117**, 11027; A. J. Arduengo, III, S. F. Gamper, M. Tamm, J. C. Calabrese, F. Davidson and H. A. Graig, *J. Am. Chem. Soc.*, 1995, **117**, 572; (*b*) A. J. Arduengo, III, S. F. Gamper, J. C. Calabrese and F. Davidson, *J. Am. Chem. Soc.*, 1994, **116**, 4391; (*c*) A. J. Arduengo, III, M. Tamm, S. J. McLain, J. C. Calabrese, F. Davidson and W. J. Marshall, *J. Am. Chem. Soc.*, 1994, **116**, 7929; H. Schumann, M. Glanz, J. Writerfield, H. Hemling, N. Kuhn and T. Kratz, *Chem. Ber.*, 1994, **127**, 2369; (*d*) W. A. Herrmann, M. Elison, J. Fischer, C. Köcher and G. R. Artus, *Angew. Chem., Int. Ed. Engl.*, 1995, **34**, 2371.

5 H.-W. Lam, G. Wilkinson, B. Hussain-Bates and M. B. Hursthouse, *J. Chem. Soc., Dalton Trans.*, 1993, 781.

6 R. I. Michelman, R. G. Bergman and R. A. Andersen, *Organometallics*, 1993, **12**, 2741.

7 W. C. Trogler, *Acc. Chem. Res.*, 1990, **23**, 426; S. W. Lee and W. C. Trogler, *Inorg. Chem.*, 1990, **29**, 1659; K. E. Meyer, P. J. Walsh and R. G. Bergmann, *J. Am. Chem. Soc.*, 1995, **117**, 974.

8 C. White, A. Yates and P. M. Maitlis, *Inorg. Synth.*, 1992, **29**, 229.

9 (*a*) C. H. Winter, S. Pirzad, D. D. Graf, D. H. Ceo and M. J. Heeg, *Inorg. Chem.*, 1993, **32**, 3654; (*b*) S. May, P. Reinsalu and J. Powell, *Inorg. Chem.*, 1980, **19**, 1582; (*c*) W. D. Jones and F. J. Feher, *Inorg. Chem.*, 1984, **23**, 2376; (*d*) P. J. Stang, Y.-H. Huang and A. M. Aref, *Organometallics*, 1992, **11**, 231.

10 A. A. Danopoulos, A. C. C. Wong, G. Wilkinson, B. Hussain-Bates and M. B. Hursthouse, *J. Chem. Soc., Dalton Trans.*, 1990, 315.

11 A.-G. Farbenfabriken Bayer, Fr. Demande, 2 000 746, 1969; *Chem. Abstr.*, 1970, **72**, 111 012m.

12 K. Baum, *J. Org. Chem.*, 1968, **33**, 4333.

13 A. A. Danopoulos, G. Wilkinson, B. Hussain-Bates and M. B. Hursthouse, *J. Chem. Soc., Dalton Trans.*, 1991, 1855.

14 G. M. Sheldrick, SHELXS 86, *Acta Crystallogr., Sect. A*, 1990, **46**, 467.

15 G. M. Sheldrick, SHELXL 93, Program for Crystal Structure Refinement, University of Göttingen, 1993.

16 N. P. C. Walker and D. Stuart, *Acta Crystallogr., Sect. A*, 1983, **39**, 158 (adapted for FAST geometry by A. Karaulov, University of Wales, Cardiff, 1991).

Received 18*th March* 1996; *Paper* 6/01850E